Published in final edited form as:
Acta Biomater. 2011 November ; 7(11): 4037–4044. doi:10.1016/j.actbio.2011.06.046.

Effects of electrospun submicron fibers in calcium phosphate cement scaffold on mechanical properties and osteogenic differentiation of umbilical cord stem cells

Chongyun Bao[1,2], **Wenchuan Chen**[1,2], **Michael D. Weir**[1], **Wahwah Thein-Han**[1], and **Hockin H. K. Xu**[1,3,4,5]

[1]Biomaterials & Tissue Engineering Division, Dept. of Endodontics, Prosthodontics and Operative Dentistry, University of Maryland Dental School, Baltimore, MD 21201, USA

[2]State Key Laboratory of Oral Diseases, West China College of Stomatology, Sichuan University, Chengdu, China

[3]Center for Stem Cell Biology & Regenerative Medicine, University of Maryland School of Medicine, Baltimore, MD 21201, USA

[4]University of Maryland Marlene and Stewart Greenebaum Cancer Center

[5]Dept. of Mechanical Engineering, University of Maryland, Baltimore County, MD 21250, USA

Abstract

Fibrous scaffolds are promising for tissue engineering because of the high surface area and fibrous features mimicking the extracellular matrix *in vivo*. Calcium phosphate cements (CPCs) can be injected and self-set in the bone defect. A literature search revealed no report on stem cell seeding on CPC containing electrospun submicron fibers. The objective of this study was to investigate the effects of electrospun fibers in CPC on mechanical properties and human umbilical cord mesenchymal stem cell (hUCMSC) proliferation, osteogenic differentiation and mineralization for the first time. Poly(D,L-lactide-*co*-glycolide) (PLGA) fibers were made via an electrospinning technique to yield an average fiber diameter of 650 nm. The fibers were incorporated into CPC consisting of tetracalcium phosphate, dicalcium phosphate anhydrous and chitosan lactate. Fiber volume fractions were 0%, 2.5%, 5% and 10%. CPC with 10% fibers had a flexural strength that was twice, and work-of-fracture (toughness) an order of magnitude, those of CPC without fibers. hUCMSCs proliferated rapidly and synthesized bone minerals while attaching to the electrospun fiber-CPC scaffolds. Alkaline phosphatase, osteocalcin, and collagen I expressions of hUCMSCs were doubled, while mineralization was increased by 40%, when fiber volume fraction in CPC was increased from 0% to 10%. The enhanced cell function was attributed to the high surface area and biomimetic features of the fiber-CPC scaffold. In conclusion, incorporating submicron fibers into CPC greatly improved the strength and toughness of CPC. Creating submicron fibrous features in CPC was a useful method for enhancing the osteogenic differentiation and mineralization of stem cells. The novel electrospun fiber-CPC-hUCMSC construct is promising for stem cell delivery and bone tissue engineering.

Corresponding author: Dr. Hockin Xu, Professor, Director of Biomaterials & Tissue Engineering Division, University of Maryland Dental School, 650 W. Baltimore St., Baltimore, MD 21201, USA. Phone: 410 706 7047. Fax: 410 706 3028. hxu@umaryland.edu.

Keywords

Electrospun Fibers; Calcium Phosphate Cement; Human Cord Stem Cells; Osteogenic Differentiation; Strength and Toughness; Bone Tissue Engineering

1. Introduction

The need for bone repair has increased as the population ages [1,2]. Seven million people suffered bone fractures in 1998 in the U. S. [3,4]. In 1995, musculoskeletal conditions cost the U. S. $215 billion [3]. These numbers are increasing rapidly as the life expectancy increases [1]. Indeed, fractures in the elderly saw a marked increase in frequency and severity [5]. Tissue engineering has the potential to meet this critical need [6-8]. Stem cell-based therapies are being actively investigated [9-13]. Human bone marrow mesenchymal stem cells (hBMSCs) have potential for bone regeneration. However, their harvest involves an invasive procedure, and their proliferation and differentiation decrease due to aging [14-16] and diseases such as osteoporosis and arthritis [17,18]. Human umbilical cord mesenchymal stem cells (hUCMSCs) are more primitive than hBMSCs. Umbilical cords are inexhaustible and can be collected at a low cost [19-22]. hUCMSCs were able to differentiate into adipocytes, osteoblasts, chondrocytes, neurons, and endothelial cells [19-26]. They exhibited a high degree of plasticity and developmental flexibility [21], caused no immunorejection and were not tumorigenic in pilot animal studies [21,22]. hUCMSCs were recently combined with calcium phosphate cement scaffolds for bone tissue engineering applications [27,28].

Electrospun fiber scaffolds have been shown to promote cell proliferation, differentiation, and mineral synthesis [29-34]. Fibrous scaffolds mimic the topology present *in vivo*, where cells reside in an extracellular matrix (ECM) composed of collagen fibers and nanoglobules [35-37]. As a result, scaffolds with nanoscale or submicron features were shown to significantly enhance cell function *in vitro* and tissue regeneration *in vivo* [38,39]. In addition, incorporation of calcium phosphate minerals to the polymer fibers yielded biomimetic scaffolds. For example, the incorporation of hydroxyapatite nanoparticles into chitosan nanofibrous scaffolds led to more bone formation compared to that of pure chitosan scaffolds [40].

Besides polymeric fibers, another important class of scaffolds for bone repair is calcium phosphate (CaP) bioceramics, with similarity to bone minerals hence good biocompatibility [41-44]. CaP implants are bioactive and can provide an ideal environment for cellular reaction and colonization by osteoblasts *in vivo*, leading to a bone-implant bonding with a functional interface [41-44]. Among CaP materials, calcium phosphate cements are highly promising because they are injectable and can self-set *in situ* to provide intimate adaptation to complex-shaped defects [45-50]. The first calcium phosphate cement (CPC) was developed in 1986 [45] and was approved in 1996 by the Food and Drug Administration (FDA) for repairing craniofacial defects in humans [47]. However, due to its brittleness and low strength, CPC is “limited to the reconstruction of non-stress-bearing bone” [46,47].

It would be highly desirable to combine electrospun fibers with CPC for the best of both worlds: The paste injectability, bioactivity and mechanical stiffness from CPC; and the high surface area for cell attachment and fiber reinforcement from the electrospun fibers. While a pile of fibers is soft and not load-bearing, once incorporated into a cement like CPC and the paste is hardened, the electrospun fibers have the potential to toughen the otherwise brittle CPC for load-bearing bone repairs. In previous studied, Vicryl suture fibers (polyglactin 910), which were poly($_{D,L}$-lactide-*co*-glycolide) (PLGA) fibers, were incorporated into CPC

[51-53]. These suture fiber bundles had diameters of 322 μm [52] and 198 μm [53], which were braided by single fibers of a diameter of 14 μm [53]. These fibers were much larger than the submicron fibers from electropspining techniques. A literature search revealed only one paper on the incorporation of electrospun fibers into CPC [54]. That study used poly(ε-caprolactone) (PCL) and poly(L-lactic acid) (PLLA) fibers which significantly increased the work-of-fracture and porosity of CPC. Cell seeding was not reported in that previous study. Therefore, the effect of incorporating electrospun submicron fibers into CPC on the stem cell proliferation and differentiation has not been reported.

Accordingly, the objective of this study was to incorporate electrospun submicron fibers into CPC and investigate hUCMSC seeding on fiber-CPC constructs for the first time. It was hypothesized that increasing the electrospun fiber volume fraction in CPC would (1) increase the load-bearing capability of the CPC scaffold; and (2) enhance the hUCMSC proliferation, osteogenic differentiation, and bone mineral synthesis on CPC.

2. Materials and methods

2.1. Development of electrospun fiber-CPC composite scaffolds

The CPC powder consisted of an mixture of tetracalcium phosphate (TTCP: $Ca_4[PO_4]_2O$) and dicalcium phosphate anhydrous (DCPA: $CaHPO_4$). TTCP was synthesized using equimolar amounts of DCPA and calcium carbonate (J.T. Baker, Philipsburg, NJ). The reactant was ground to obtain TTCP particles of 1 to 80 μm, with a median of 17 μm. DCPA was ground to obtain a median particle size of 1 μm. TTCP and DCPA powders were mixed at a molar ratio of 1:1 to form the CPC powder. Chitosan lactate (VANSON, Redmond, WA) was mixed with water at a chitosan/(chitosan + water) mass fraction of 15% to form the CPC liquid. The incorporation of chitosan into CPC could not only impart fast-setting and washout resistance to the CPC paste, but also improve the mechanical properties of CPC [49,55]. All the scaffolds in the present study were made using the chitosan liquid.

Submicron fibers of poly(D,L-lactide-*co*-glycolide) (PLGA) at a poly(lactic acid) (PLA) to poly(glycolic acid) (PGA) ratio of 50:50 were electrospun into a non-woven mat, based on parameters from previous studies [56,57]. Briefly, a 10% by weight polymer solution of PLGA (inherent viscosity = 0.8-1.2; PolySciences, Warrington, PA) was prepared in a binary mixture of (1:3) dimethylformamide (DMF) and dichloromethane (DCM) (Sigma-Aldrich) and allowed to dissolve for 24 h with constant stirring. The solution was placed into a 10 mL syringe fitted with a 21-gauge needle. The syringe was fixed vertically into a syringe pump 12.5 cm from an aluminum collecting plate. A voltage of 13 kV was applied using a high voltage power supply (Gamma High Voltage, Ormond Beach, FL), with the electric field existing between the aluminum collecting plate (cathode) and the needle tip (anode). The polymer solution was pumped from the syringe at a flow rate of 0.6 mL/h and a non-woven mat was formed on the collection plate. The fiber mat was cut into 3 mm × 3 mm squares using a sharp razor blade and a ruler, because a previous study showed that 3-mm fibers mixed in the CPC paste was injectable through a 10-gauge needle [28]. In addition, another previous study also cut the electrospun fibers into 3-mm dimensions for use in calcium phosphate cement [54]. The CPC powder and chitosan liquid was mixed at a mass ratio of 2:1. Then the fibers were mixed with CPC-chitosan paste to form a cohesive paste. For each specimen, the mixing was done with a spatula on a flat glass slab. The fibers were randomly mixed with the CPC paste for approximately half a minute, and then the paste was placed into a stainless steel mold of 3 × 4 × 25 mm, following previous studies [49,51,52]. The following fiber volume fractions (fiber volume/specimen volume) were tested: 0%, 2.5%, 5%, and 10%. Fiber volume fractions larger than 10% were not used as the paste was not flowable for injection applications. The specimens were incubated in a humidor at 37 °C for four hours. While the initial setting of CPC-chitosan took about 7

minutes [49], the 4-hour incubation was done for the CPC to develop sufficient strength to withstand the forces needed to push the specimen out of the mold. The specimens were demolded and immersed in a simulated physiological solution (1.15 mmol/L Ca, 1.2 mmol/L P, 133 mmol/L NaCl, 50 mmol/L HEPES, buffered to a pH of 7.4) for 20 hours prior to mechanical testing.

The electrospun fibers and scaffolds were sputter coated with gold and examined in a scanning electron microscope (SEM, FEI Quanta 200, Hillsboro, OR). The fiber diameters were measured, and the fiber distribution in CPC and bonding with CPC were examined.

2.2. Mechanical testing

A three-point flexural test was used to fracture the specimens on a Universal Testing Machine (MTS, Eden Prairie, MN) using a span of 20 mm at a crosshead speed of 1 mm/min [28]. Flexural strength, $S = 3F_{max}L/(2bd^2)$, where F_{max} is the maximum load on the load-displacement (F-c) curve, L is span, b is specimen width, and d is specimen thickness. Elastic modulus $E = (F/c)\,(L^3/[4bd^3])$. Work-of-fracture (toughness) is the area under the F-c curve divided by the specimen's cross-sectional area.

2.3. hUCMSC viability on electrospun fiber-CPC scaffolds

hUCMSCs were obtained commercially (ScienCell, Carlsbad, CA). Cells were harvested from the Wharton's jelly of umbilical cords of healthy babies born at normal term as described previously [24,26]. The use of hUCMSCs was approved by the University of Maryland. hUCMSCs were cultured in a low-glucose Dulbecco's modified Eagle's medium (DMEM, Catalog No. 11885-084) with 10% Dulbecco's phosphate-buffered saline (DPBS) and 1% penicillin/streptomycin (PS) (Invitrogen, Carlsbad, CA) (control media). Passage 4 hUCMSCs were used. The osteogenic media contained 100 nM dexamethasone, 10 mM β-glycerophosphate, 0.05 mM ascorbic acid, and 10 nM 1α,25-Dihydroxyvitamin (Sigma) [28]. The osteogenic media was used for all the cell experiments, including the live-dead assay, osteogenic differentiation, and mineral staining experiments. Following a previous study [58], 150,000 cells were diluted into 2 mL of osteogenic media and added to each well containing a CPC disk of 2 mm in thickness and 12 mm in diameter, using 24-well plates. After 1, 4, and 8 days [58], the media was removed and the cells were washed in Tyrode's Hepes buffer. Cells were live/dead stained and viewed by epifluorescence microscopy (TE300, Nikon, Melville, NY). Three randomly-chosen fields of view were photographed from each disk (five disks yielded 15 photos per material). The cells were counted. N_{Live} is the number of live cells, and N_{Dead} is the number of dead cells. The percentage of live cells, $P = N_{Live}/(N_{Live} + N_{Dead})$. The live cell density, D, was the number of live cells divided by the area, A: $D = N_{Live}/A$ [59].

2.4. Osteogenic differentiation of hUCMSCs on electrospun fiber-CPC scaffolds

Osteogenic differentiation of hUCMSCs attaching on fiber-CPC were measured using quantitative real-time reverse transcription polymerase chain reaction (qRT-PCR, 7900HT, Applied Biosystems, Foster City, CA) [59]. The total cellular RNA of the cells were extracted with TRIzol reagent (Invitrogen) and reverse-transcribed into cDNA using a High-Capacity cDNA Archive kit. TaqMan gene expression kits were used to measure the transcript levels of the proposed genes on human alkaline phosphatase (ALP, Hs00758162_m1), osteocalcin (OC, Hs00609452_g1), collagen type I (Coll I, Hs00164004), and glyceraldehyde 3-phosphate dehydrogenase (GAPDH, Hs99999905). Relative expression for each target gene was evaluated using the $2^{-\Delta\Delta Ct}$ method [60]. Ct values of target genes were normalized by the Ct of the TaqMan human housekeeping gene GAPDH to obtain the ΔCt values. The Ct of hUCMSCs cultured on tissue culture polystyrene in control media for 1 d served as the calibrator [28,58].

2.5. hUCMSC mineralization on electrospun fiber-CPC scaffolds

hUCMSCs were seeded on CPC disks and cultured in osteogenic media for 7, 14 and 21 d. The samples were then fixed with 10% formaldehyde and stained with Alizarin Red S (ARS) (Millipore, Billerica, MA), which stained calcium-rich deposits by cells into a red color. An osteogenesis assay (Millipore) was used to extract the stained minerals and measure the Alizarin Red concentration following the manufacture's instructions. Control scaffolds with the same compositions, but without hUCMSCs, were also measured at the same time periods and received the same treatments except without the cells. The control's Alizarin Red concentration was subtracted from the Alizarin Red concentration of the corresponding scaffold with hUCMSCs, to yield the net mineral concentration synthesized by the cells. The time periods of up to 21 d were selected because previous studies found a large increase in calcium content during *in vitro* cell cultures from 12 d to 21 d [61].

One-way and two-way ANOVA were performed to detect significant ($\alpha = 0.05$) effects of the variables. Tukey's multiple comparison procedures were used to group and rank the measured values, and Dunn's multiple comparison tests were used on data with non-normal distribution or unequal variance, both at a family confidence coefficient of 0.95.

3. Results

Fig. 1 shows SEM micrographs of the electrospun PLGA fibers at (A) low, and (B) high magnification. The fibers were long and continuous, and were generally separate from each other. Occasionally, fibers appeared to be fused at the intersections (arrow in B). The diameters were measured for 120 fibers. The diameters ranged from about 300 nm to 900 nm, with an average diameter of 650 nm.

The mechanical properties vs. the electrospun fiber volume fraction in CPC are plotted in Fig. 2. In each plot, values indicated with dissimilar letters are significantly different from each other ($p < 0.05$). In (A), the flexural strength (mean ± sd; $n = 6$) at 10% fibers was 2-fold that of CPC control without fibers. Work-of-fraction was increased by an order of magnitude when the fiber content was increased from 0% to 10%. Elastic moduli in (C) were not significantly increased due to fiber addition ($p > 0.1$), as the PLGA fibers were flexible and not stiff.

The fractured bars were viewed via SEM on their cross sections to examine the interior of the specimens. Fig. 3 shows SEM micrographs of typical CPC cross-sectional surfaces with fiber volume fractions of (A) 0%, (B) 2.5%, (C) 5%, and (D) 10%. In the CPC without fibers, the micron-sized and submicron-sized pores were the intrinsic porosity because the chitosan liquid contained water. The fiber density in the CPC noticeably increased with higher fiber content. The fibers appeared to be mingled well with the CPC paste, with CPC separating the neighboring fibers, and with fibers orienting in different directions. There appeared to be fiber-CPC bonding, manifested by numerous CPC remnants (arrows) that were still attaching to the fibers after the fibers were pulled out of the CPC matrix when the bar was fractured.

Live/dead photos of hUCMSCs on fiber-CPC are shown in Fig. 4. Live cells were stained green and were numerous. Dead cells were stained a red/orange color and were few (arrows indicate examples). Comparing 1 d with 8 d, it is obvious that the hUCMSCs on fiber-CPC had greatly proliferated. For CPC with different fiber volume fractions, it can be seen that CPC with 10% fibers had more cells than CPC without fibers.

Fig. 5 plots (A) the percentage of live cells P, and (B) the live cell density D. In (A), increasing the culture time from 1 d to 8 d increased P from 79% to 97% ($p < 0.05$). In (B),

increasing the fiber content in CPC increased the cell density. At 4 d, the cell density on CPC with 5% and 10% fibers was higher than that without fibers ($p < 0.05$). At 8 d, the cell density on CPC with 10% fibers was higher than all other values ($p < 0.05$). The hUCMSC proliferation increased D, from about 100 cells/mm^2 at 1 d to 700 cells/mm^2 at 8 d ($p < 0.05$). This indicates a 7-fold increase in hUCMSC density in a week.

The osteogenic differentiation results are plotted in Fig. 6. ALP at 8 d was higher for hUCMSCs on CPC with fibers than that without fibers ($p < 0.05$). OC was the highest for CPC with 10% fibers at 1 d and 4 d, than all other groups. At 8 d, OC was higher for hUCMSCs on CPC with fibers than that without fibers ($p < 0.05$). Collagen I was higher with 5% and 10% fibers than that without fibers, at both 4 d and 8 d. Therefore, adding PLGA fibers to CPC increased the osteogenic gene expressions of the hUCMSCs.

The ARS staining of mineralization by the hUCMSCs are shown in Fig. 7. There was little mineralization by the cells at 7 d. The ARS mineral staining yielded a bright red color for the CPC matrix, as the CPC was made up of hydroxyapatite minerals. The “no cell” control disks were also incubated in the medium for the same time periods up to 21d and received the same treatment except without the cells. Their images (not included) were very similar to those with cells at 7 d with 0% fibers and 2.5% fibers in Fig. 7. The cell mineralization increased at 14 d and 21 d. At the same time period, the mineralization increased with higher fiber volume fraction in CPC. This was manifested by the staining becoming thicker and denser, and the amount of cell deposits increasing with culture time and fiber content. Data from the osteogenesis assay are shown in the plot. The mineral amount increased with culture time ($p < 0.05$), and with fiber content ($p < 0.05$). At 14 d and 21 d, the mineral amounts for CPC with fibers were higher than that without fibers ($p < 0.05$). At 21 d, the mineral amount with 10% fibers was higher than that with 2.5% fibers ($p < 0.05$). Hence, hUCMSCs seeded on fiber-CPC scaffolds were differentiated into the osteogenic lineage, and cell mineralization was enhanced by incorporating PLGA fibers into CPC.

4. Discussion

The present study represents the first report on stem cell seeding on CPC containing electrospun submicron fibers. The effects of fiber volume fraction in CPC on cell proliferation, osteogenic differentiation, and mineralization were determined. Previous studies were performed on electrospun fibers for tissue engineering because fibrous scaffolds mimic the collagen fiber-containing extracellular matrix (ECM) [29-37]. Many studies focused on electrospun polymeric fibers such as microporous, non-woven poly (epsilon-caprolactone) (PCL) [29,35], poly(lactic acid) (PLA)-gelatin, and electrospinning of collagen onto starch-based fiber meshes [36]. Other studies developed bioceramic/polymer composite fibers to combine the bioactivity and hydrophilicity of bioceramics [31,33,34,40] with the toughness of polymers. Examples include hydroxyapatite-chitosan fibers [40], poly[bis(ethyl alanato)phosphazene]-hydroxyapatite fibers [31], and hydroxyapatite-collagen-chitosan fibers [33]. The addition of a bioceramic component such as CaP to the polymer fibers induced better cell proliferation and enhanced mineralization and alkaline phosphatase activity (ALP) [32], and resulted in more new bone formation in animal models [34]. This is likely because adding calcium phosphate minerals to the fibers yielded a biomimetic matrix, as the bone ECM consists of submicron fibrous features as well as calcium phosphate minerals.

Injectable CPCs are a promising matrix for the development of scaffolds with submicron fibrous features, as various compositions and amounts of fibers can be readily mixed into the CPC paste. The CPC provides bioactivity while the fibers provide reinforcement and increased surface area to enhance cell attachment. Indeed, in a recent study, reinforcement

via electrospun fibers increased the work-of-fracture of a calcium phosphate cement by an order of magnitude [54]. In the present study, the flexural strength of the CPC containing 10% fibers was 2-fold that without fibers, while the work-of-fracture was increased by nearly 10-fold. A previous study reported that an injectable polymeric carrier for cell delivery had a compressive strength of about 0.7 MPa [62]. Other studies reported that hygrogels for cell delivery had a tensile strength of about 0.07 MPa [63,64]. While these novel materials are promising for tissue engineering, it was rightfully concluded that "Hydrogel scaffolds are used in nonload bearing bone tissue engineering. … They do not possess the mechanical strength to be used in load bearing applications" [64]. In comparison, the electrospun fiber-CPC at 5-10% fibers had flexural strengths of 7-10 MPa, which are more than an order of magnitude higher than the reported injectable polymers and hydrogels for cell delivery. Therefore, the fiber-CPC scaffold may be useful for stem cell delivery in a wide range of load-bearing orthopedic and craniofacial applications. Previous studies showed that the PLGA suture fibers could provide the needed early-strength to the CPC implant for approximately one to two months, and then the fibers degraded [49,52,53]. The fiber degradation increased the porosity in the CPC scaffold which could enhance cell infiltration and tissue ingrowth [49,52]. Further study is needed to investigate the degradation of the electrospun PLGA fibers in a CPC scaffold *in vivo*.

Besides improving the strength and toughness, incorporating electrospun submicron fibers into CPC was demonstrated to increase stem cell proliferation, osteogenic differentiation and mineralization, for the first time. hUCMSCs attaching to the CPC with 10% fibers had ALP, OC and collagen I gene expressions about 2-fold those on CPC without fibers. Cell mineralization was increased by about 40% when the fiber volume fraction in CPC was increased from 0% to 10%. In our previous study using the same hUCMSCs from the same commercial source, the substance synthesized by hUCMSCs, similar to those deposited on the surfaces of the disks in Fig. 7, were collected and examined via x-ray diffraction (XRD) [59]. The XRD pattern of the hUCMSC-synthesized substance matched that of a known hydroxyapatite control, confirming that the cell-synthesized substance was an apatitic mineral [59]. In addition, the cell-synthesized substance was dissolved in an acetic acid solution which was measured via a spectrophotometric method. This yielded a Ca/P molar ratio of 1.35 [59]. This ratio was consistent with the previously-reported Ca/P ratios ranging of about 1.39 and 1.41 for minerals deposited by rat dental pulp cells [65].

The mechanism of the observed enhancement in cell function is likely related to the increased surface area and roughness of the fibrous scaffolds. A recent study showed a 3-fold greater bone tissue ingrowth in defects containing carbon-nanotube nanocomposite scaffold, compared to control polymer scaffolds without nanotubes [38]. These results suggest that nanotubes may render nanocomposite scaffolds bioactive assisting osteogenesis [38], which was related to the nanostructure with a high surface area and roughness. This in turn enhanced cell attachment, and might also absorb more proteins and bioactive molecules *in vivo* to stimulate the cells and accelerate the synthesis of an ECM. This is consistent with another study, which showed that cells on chitosan nanofibers exhibited better viability and adhesion, and secreted 1.5-2 fold more proteins, than cells on regular chitosan film without nano-features [39]. Therefore, for the present study, it would be interesting to estimate the specific surface area of the electrospun fibers. For fibers with a length much larger than the diameter (*e.g.*, 3 mm fiber length vs. 650 nm diameter), the cross sectional area at the two ends of a single fiber can be neglected, and the fiber surface area $A = \pi D \cdot L$, where D is fiber diameter and L is fiber length. For a pile of such fibers, the fiber specific surface area (the total fiber surface area divided by the total fiber mass) is $S = 4/(D \cdot \rho)$, where ρ is fiber density (mass/volume). Therefore, the specific surface area is inversely proportional to the fiber diameter. Assume that the PLGA fibers in the previous studies [52,53] and the PLGA fibers in the present study have approximately the same density, then $S_{electrospun}/S_{suture} =$

$D_{suture}/D_{electrospun}$ = 462. $S_{electrospun}$ is the specific surface area of the electrospun fibers of the present study with diameter $D_{electrospun}$ of 650 μm (= 0.65 μm). S_{suture} is the specific surface area of the suture fiber bundle of previous studies with diameter D_{suture} of approximately 300 μm. Hence, the electrospun fibers of the present study had a specific surface area 462-fold that of the previous suture fibers. Furthermore, the suture bundle was braided using single fibers of a diameter of D_{single} = 14 μm. Hence, $S_{electrospun}/S_{single}$ = $D_{single}/D_{electrospun}$ = 22. The electrospun fibers of the present study had a specific surface area that was 22-fold that of the single fiber inside the suture. Therefore, the electrospun submicron fibers of the present study had a specific surface area that was orders of magnitude higher than previous PLGA fibers used in CPC [52,53]. Hence, the mechanism for enhancing the hUCMSC function in the present study was likely that the high surface area of the electrospun submicron fibers enhanced the hUCMSC spreading and viability, resulting in a higher proliferation and cell density (Fig. 5B). Furthermore, the fibers mimic the fibrous topology of the extracellular matrix *in vivo*, which may have contributed to the increased osteogenic gene expressions and mineralization for the hUCMSCs (Figs. 6 and 7). While incorporating fibers into CPC was advantageous, the mixing of CPC paste with fibers was relatively easy when using a CPC powder to liquid ratio of 2 to 1, which formed a flowable paste. A previous study showed that the composite mechanical properties were not significantly different from each other when the fiber-CPC mixing was performed by three different operators: one with extensive mixing experience, one with a little mixing experience, and one with no mixing experience [66]. Further animal study is needed to investigate if the hUCMSC-fiber-CPC construct would generate more new bone tissue than that without the electrospun fibers.

5. Conclusions

This study incorporated electrospun submicron PLGA fibers into a self-setting CPC and investigated stem cell proliferation and osteogenic differentiation on fiber-CPC for the first time. Increasing the fiber volume fraction increased the hUCMSC proliferation, osteogenic expressions and mineralization. The electrospun fibers increased the flexural strength of CPC by 2-fold, and toughness by an order of magnitude. The strength of fiber-CPC was an order of magnitude the reported strengths of polymers and hydrogels for cell delivery. When the fiber volume fraction in CPC was increased from 0% to 10%, the ALP, OC and collagen I expressions of hUCMSCs were doubled, while mineralization was increased by nearly 40%. The related mechanism was attributed to the high surface area and biomimetic features of the electrospun fiber-CPC scaffold. Therefore, imparting submicron-scale fibrous features to CPC, via the incorporation of electrospun fibers, appeared to be a useful method to enhance the osteogenic differentiation and mineralization of stem cells. The strong and tough fiber-CPC-hUCMSC construct with excellent proliferation and osteogenic differentiation may be useful for a wide range of load-bearing orthopedic applications.

Acknowledgments

We are grateful to Dr. Laurence C. Chow and Dr. Shozo Takagi at the Paffenbarger Research Center and Dr. Carl G. Simon at the National Institute of Standards and Technology for discussions. We thank Prof. Xuedong Zhou and Prof. Qianming Chen of the West China College of Stomatology for support. This study was funded by NIH grants R01 DE14190 and DE17974 (HX), Maryland Stem Cell Fund 2008-MSCRFE-0109 (HX), the University of Maryland Dental School, and State Key Laboratory of Oral Diseases of West China College of Stomatology.

References

1. Laurencin CT, Ambrosio AMA, Borden MD, Cooper JA. Tissue engineering: Orthopedic applications. Annual Rev Biomed Eng. 1999; 1:19–46. [PubMed: 11701481]

2. Bohner M. Design of ceramic-based cements and putties for bone graft substitution. Eur Cell Mater. 2010; 20:1–12. [PubMed: 20574942]

3. Praemer, A.; Furner, S.; Rice, DP. Musculoskeletal conditions in the United States. Vol. chapter 1. Rosemont, IL: Am Acad Orthop Surg; 1999.

4. Medical Data International. RP-651147 - Orthopedic and musculoskeletal markets: Biotechnology and tissue engineering. Irvine, CA: Medical Data Intl; 2000. p. 28-31.

5. An, YH. Internal fixation in osteoporotic bone. New York, NY: Thieme Medical; 2002. Foreword

6. Ginebra MP, Traykova T, Planell JA. Calcium phosphate cements as bone drug-delivery systems: a review. J Controlled Release. 2006; 113:102–110.

7. Johnson PC, Mikos AG, Fisher JP, Jansen JA. Strategic directions in tissue engineering. Tissue Eng. 2007; 13:2827–2837. [PubMed: 18052823]

8. Mao, JJ.; Vunjak-Novakovic, G.; Mikos, AG.; Atala, A. Regenerative medicine: Translational approaches and tissue engineering. Vol. Chapters 1-3. Boston, MA: Artech House; 2007.

9. Salgado AJ, Coutinho OP, Reis RL. Bone tissue engineering: state of the art and future trends. Macromol Biosci. 2004; 4:743–765. [PubMed: 15468269]

10. Gomes, ME.; Mikos, AG.; Reis, RL. Injectable polymeric scaffolds for bone tissue engineering. In: Reis, RL.; San Roman, J., editors. Biodegradable systems in tissue engineering and regenerative medicine. Boca Raton, FL: CRC Press; 2004. p. 29-38.

11. Mao JJ, Giannobile WV, Helms JA, Hollister SJ, Krebsbach PH, Longaker MT, et al. Craniofacial tissue engineering by stem cells. J Dent Res. 2006; 85:966–979. [PubMed: 17062735]

12. Salinas CN, Anseth KS. The influence of the RGD peptide motif and its contextual presentation in PEG gels on human mesenchymal stem cell viability. J Tissue Eng Regen Med. 2008; 2:296–304. [PubMed: 18512265]

13. Benoit DS, Schwartz MP, Durney AR, Anseth KS. Small functional groups for controlled differentiation of hydrogel-encapsulated human mesenchymal stem cells. Nat Mater. 2008; 7:816–823. [PubMed: 18724374]

14. Mueller SM, Glowacki J. Age-related decline in the osteogenic potential of human bone marrow cells cultured in three-dimensional collagen sponges. J Cell Biochem. 2001; 82:583–590. [PubMed: 11500936]

15. Mendes SC, Tibbe JM, Veenhof M, Bakker K, Both S, Platenburg PP, et al. Bone tissue-engineered implants using human bone marrow stromal cells: Effect of culture conditions and donor age. Tissue Eng. 2002; 8:911–920. [PubMed: 12542937]

16. Stenderup K, Justesen J, Clausen C, Kassem M. Aging is associated with decreased maximal life span and accelerated senescence of bone marrow stromal cells. Bone. 2003; 33:919–926. [PubMed: 14678851]

17. Rodriguez JP, Montecinos L, Rios S, Reyes P, Martinez J. Mesenchymal stem cells from osteoporotic patients produce a type I collagen-deficient extracellular matrix favoring adipogenic differentiation. J Cell Biochem. 2000; 79:557–565. [PubMed: 10996846]

18. Suzuki Y, Kim KJ, Kotake S, Itoh T. Stromal cell activity in bone marrow from the tibia and iliac crest of patients with rheumatoid arthritis. J Bone Miner Metab. 2001; 19:56–60. [PubMed: 11156475]

19. Wang HS, Hung SC, Peng ST. Mesenchymal stem cells in the Wharton's jelly of the human umbilical cord. Stem Cells. 2004; 22:1330–1337. [PubMed: 15579650]

20. Sarugaser R, Lickorish D, Baksh D, Hosseini MM, Davies JE. Human umbilical cord perivascular (HUCPV) cells: A source of mesenchymal progenitors. Stem Cells. 2005; 23:220–229. [PubMed: 15671145]

21. Weiss ML, Medicetty S, Bledsoe AR, Rachakatla RS, Choi M, Merchav S, et al. Human umbilical cord matrix stem cells: Preliminary characterization and effect of transplantation in a rodent model of Parkinson's disease. Stem Cells. 2006; 24:781–792. [PubMed: 16223852]

22. Can A, Karahuseyinoglu S. Concise review: Human umbilical cord stroma with regard to the source of fetus-derived stem cells. Stem Cells. 2007; 25:2886–2895. [PubMed: 17690177]

23. Baksh D, Yao R, Tuan RS. Comparison of proliferative and multilineage differentiation potential of human mesenchymal stem cells derived from umbilical cord and bone marrow. Stem Cells. 2007; 25:1384–1392. [PubMed: 17332507]

24. Bailey MM, Wang L, Bode CJ, Mitchell KE, Detamore MS. A comparison of human umbilical cord matrix stem cells and temporomandibular joint condylar chondrocytes for tissue engineering temporomandibular joint condylar cartilage. Tissue Eng. 2007; 13:2003–2010. [PubMed: 17518722]
25. Jäger M, Degistirici O, Knipper A, Fischer J, Sager M, Krauspe R. Bone healing and migration of cord blood-derived stem cells into a critical size femoral defect after xenotransplantation. J Bone Miner Res. 2007; 22:1224–1233. [PubMed: 17451370]
26. Wang L, Singh M, Bonewald LF, Detamore MS. Signaling strategies for osteogenic differentiation of human umbilical cord mesenchymal stromal cells for 3D bone tissue engineering. J Tissue Eng Regen Med. 2009; 3:398–404. [PubMed: 19434662]
27. Xu HHK, Zhao L, Detamore MS, Takagi S, Chow LC. Umbilical cord stem cell seeding on fast-resorbable calcium phosphate bone cement. Tissue Engineering Part A. 2010; 16:2743–2753. [PubMed: 20388037]
28. Zhao L, Weir MD, Xu HHK. An injectable calcium phosphate - alginate hydrogel -umbilical cord mesenchymal stem cell paste for bone tissue engineering. Biomaterials. 2010; 31:6502–6510. [PubMed: 20570346]
29. Yoshimoto H, Shin YM, Terai H, Vacanti JP. A biodegradable nanofiber scaffold by electrospinning and its potential for bone tissue engineering. Biomaterials. 2003; 24:2077–2082. [PubMed: 12628828]
30. Wei G, Jin Q, Giannobile WV, Ma PX. The enhancement of osteogenesis by nanofibrous scaffolds incorporating rhBMP-7 nanospheres. Biomaterials. 2007; 28:2087–2096. [PubMed: 17239946]
31. Bhattacharyya S, Kumbar SG, Khan YM, Nair LS, Singh A, Krogman NR, et al. Biodegradable polyphosphazene-nanohydroxyapatite composite nanofibers: scaffolds for bone tissue engineering. J Biomed Nanotechnol. 2009; 5:69–75. [PubMed: 20055108]
32. Gupta D, Venugopal J, Mitra S, Giri VR, Ramakrishna S. Nanostructured biocomposite substrates by electrospinning and electrospraying for the mineralization of osteoblasts. Biomaterials. 2009; 30:2085–2094. [PubMed: 19167752]
33. Zhang Y, Reddy VJ, Wong SY, Li X, Su B, Ramakrishna S, et al. Enhanced biomineralization in osteoblasts on a novel electrospun biocomposite nanofibrous substrate of hydroxyapatite/collagen/chitosan. Tissue Eng Part A. 2010; 16:1949–1960. [PubMed: 20088700]
34. Nandakumar A, Yang L, Habibovic P, van Blitterswijk C. Calcium phosphate coated electrospun fiber matrices as scaffolds for bone tissue engineering. Langmuir. 2010; 26:7380–7387. [PubMed: 20039599]
35. Wang J, Valmikinathan CM, Liu W, Laurencin CT, Yu X. Spiral-structured, nanofibrous, 3D scaffolds for bone tissue engineering. J Biomed Mater Res A. 2010; 93:753–62. [PubMed: 19642211]
36. Tuzlakoglu K, Santos MI, Neves N, Reis RL. Design of nano- and microfiber combined scaffolds by electrospinning of collagen onto starch-based fiber meshes: a man-made equivalent of natural extracellular matrix. Tissue Eng Part A. 2011; 17:463–473. [PubMed: 20825361]
37. Hu J, Liu X, Ma PX. Induction of osteoblast differentiation phenotype on poly(L-lactic acid) nanofibrous matrix. Biomaterials. 2008; 29:3815–3821. [PubMed: 18617260]
38. Sitharaman B, Shi X, Walboomers XF, Liao H, Cuijpers V, Wilson LJ, et al. *In vivo* biocompatibility of ultra-short single-walled carbon nanotube/biodegradable polymer nanocomposites for bone tissue engineering. Bone. 2008; 43:362–370. [PubMed: 18541467]
39. Chu XH, Shi XL, Feng ZQ, Gu ZZ, Ding YT. Chitosan nanofiber scaffold enhances hepatocyte adhesion and function. Biotechnol Let. 2009; 31:347–352. [PubMed: 19037598]
40. Zhang Y, Venugopal JR, El-Turki A, Ramakrishna S, Su B, Lim CT. Electrospun biomimetic nanocomposite nanofibers of hydroxyapatite/chitosan for bone tissue engineering. Biomaterials. 2008; 29:4314–4322. [PubMed: 18715637]
41. Ducheyne P, Qiu Q. Bioactive ceramics: The effect of surface reactivity on bone formation and bone cell function. Biomaterials. 1999; 20:2287–2303. [PubMed: 10614935]
42. Ginebra MP, Rilliard A, Fernández E, Elvira C, Román JS, Planell JA. Mechanical and rheological improvement of a calcium phosphate cement by the addition of a polymeric drug. J Biomed Mater Res. 2001; 57:113–118. [PubMed: 11416857]

43. Ginebra MP, Driessens FCM, Planell JA. Effect of the particle size on the micro and nanostructural features of a calcium phosphate cement: a kinetic analysis. Biomaterials. 2004; 25:3453–3462. [PubMed: 15020119]
44. Kasten P, Beyen I, Niemeyer P, Luginbuhl R, Bohner M, Richter W. Porosity and pore size of beta-tricalcium phosphate scaffold can influence protein production and osteogenic differentiation of human mesenchymal stem cells: an *in vitro* and *in vivo* study. Acta Biomater. 2008; 4:1904–1915. [PubMed: 18571999]
45. Brown, WE.; Chow, LC. A new calcium phosphate water setting cement. In: Brown, PW., editor. Cements research progress. Westerville, OH: Am Ceram Soc; 1986. p. 352-379.
46. Shindo ML, Costantino PD, Friedman CD, Chow LC. Facial skeletal augmentation using hydroxyapatite cement. Arch Otolaryngol Head Neck Surg. 1993; 119:185–190. [PubMed: 8427682]
47. Friedman CD, Costantino PD, Takagi S, Chow LC. BoneSource hydroxyapatite cement: a novel biomaterial for craniofacial skeletal tissue engineering and reconstruction. J Biomed Mater Res B. 1998; 43:428–432.
48. Barralet JE, Gaunt T, Wright AJ, Gibson IR, Knowles JC. Effect of porosity reduction by compaction on compressive strength and microstructure of calcium phosphate cement. J Biomed Mater Res B. 2002; 63:1–9.
49. Xu HHK, Takagi S, Quinn JB, Chow LC. Fast-setting and anti-washout calcium phosphate scaffolds with high strength and controlled macropore formation rates. J Biomed Mater Res. 2004; 68A:725–734.
50. Bohner M, Baroud G. Injectability of calcium phosphate pastes. Biomaterials. 2005; 26:1553–1563. [PubMed: 15522757]
51. Xu HHK, Eichmiller FC, Giuseppetti AA. Reinforcement of a self-setting calcium phosphate cement with different fibers. J Biomed Mater Res. 2000; 52:107–114. [PubMed: 10906680]
52. Xu HHK, Quinn JB. Calcium phosphate cement containing resorbable fibers for short-term reinforcement and macroporosity. Biomaterials. 2002; 23:193–202. [PubMed: 11763861]
53. Guo D, Sun H, Xu K, Han Y. Long-term variations in mechanical properties and in vivo degradation of CPC/PLGA composite. J Biomed Mater Res B. 2007; 82:533–544.
54. Zuo Y, Yang F, Wolke JG, Li Y, Jansen JA. Incorporation of biodegradable electrospun fibers into calcium phosphate cement for bone regeneration. Acta Biomaterialia. 2010; 6:1238–1247. [PubMed: 19861181]
55. Takechi M, Miyamoto Y, Ishikawa K, Yuasa M, Nagayama M, Kon M, Asaoka K. Non-decay type fast-setting calcium phosphate cement using chitosan. J Mater Sci Mater Med. 1996; 7:317–322.
56. Li WJ, Cooper JA, Mauck RL, Tuan RS. Fabrication and characterization of six electrospun poly(alpha-hydroxy ester)-based fibrous scaffolds for tissue engineering applications. Acta Biomaterialia. 2006; 2:377–385. [PubMed: 16765878]
57. Yoon OJ, Kim HW, Kim DJ, Lee HJ, Yun JY, Noh YH, et al. Nanocomposites of electrospun poly[(d,l-lactic)-co(glycolic acid)] and plasma-functionalized single-walled carbon nanotubes for biomedical applications. Plasma Process Polym. 2009; 6:101–109.
58. Kim K, Dean D, Mikos AG, Fisher JP. Effect of initial cell seeding density on early osteogenic signal expression of rat bone marrow stromal cells cultured on cross-linked poly(propylene fumarate) disks. Biomacromolecules. 2009; 10:1810–1817. [PubMed: 19469498]
59. Xu HHK, Zhao L, Weir MD. Stem cell-calcium phosphate constructs for bone engineering. J Dent Res. 2010; 89:1482–1488. [PubMed: 20929721]
60. Livak KJ, Schmittgen TD. Analysis of relative gene expression data using real-time quantitative PCR and the $2^{-\Delta\Delta Ct}$ method. Methods. 2001; 25:402–408. [PubMed: 11846609]
61. Wang YH, Liu Y, Maye P, Rowe DW. Examination of mineralized nodule formation in living osteoblastic cultures using fluorescent dyes. Biotechnol Prog. 2006; 22:1697–701. [PubMed: 17137320]
62. Shi X, Sitharaman B, Pham QP, Liang F, Wu K, Billups WE, et al. Fabrication of porous ultra-short single-walled carbon nanotube nanocomposite scaffolds for bone tissue engineering. Biomaterials. 2007; 28:4078–4090. [PubMed: 17576009]

63. Kuo CK, Ma PX. Ionically crosslinked alginate hydrogels as scaffolds for tissue engineering: Part I. Structure, gelation rate and mechanical properties. Biomaterials. 2001; 22:511–521. [PubMed: 11219714]

64. Drury JL, Dennis RG, Mooney DJ. The tensile properties of alginate hydrogels. Biomaterials. 2004; 25:3187–3199. [PubMed: 14980414]

65. Nakamura H, Saruwatari L, Aita H, Takeuchi K, Ogawa T. Molecular and biomechanical characterization of mineralized tissue by dental pulp cells on titanium. J Dent Res. 2005; 84:515–520. [PubMed: 15914587]

66. Xu HHK, Simon CG Jr, Takagi S, Chow LC, Eichmiller FC. Strong, macroporous and in-situ hardening hydroxyapatite for bone tissue engineering. Biomaterials Forum. 2005; 27:14–19.

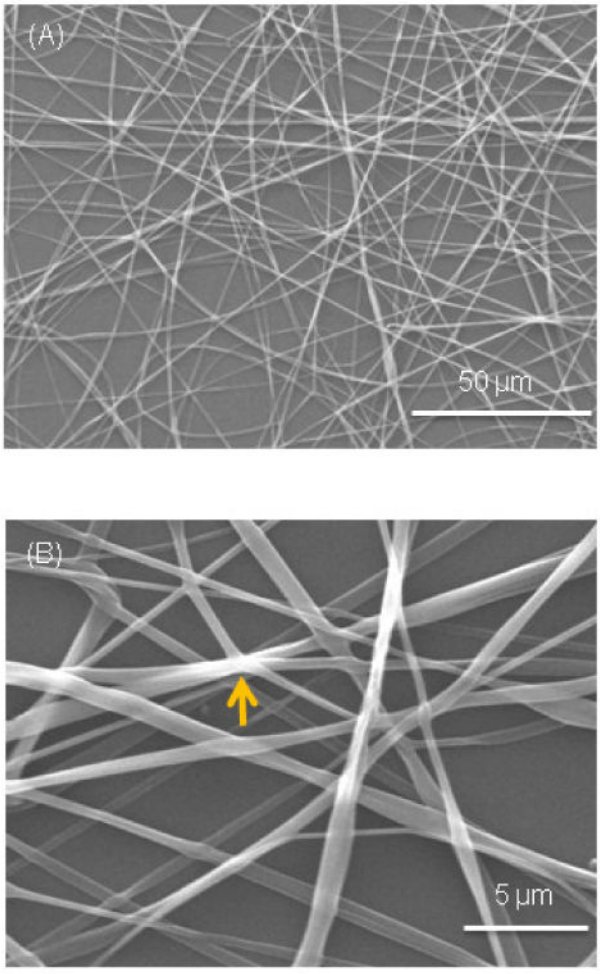

[1].

Typical SEM micrographs of submicron PLGA fibers electrospun in this study, shown at (A) low, and (B) high magnification. The fibers were mostly continuous and separate from each other. Arrows in (B) indicate occasional fibers that appeared to be fused at the intersections. These fibers were of poly(D,L-lactide-*co*-glycolide) (PLGA) at a poly(lactic acid) (PLA) to poly(glycolic acid) (PGA) ratio of 50:50.

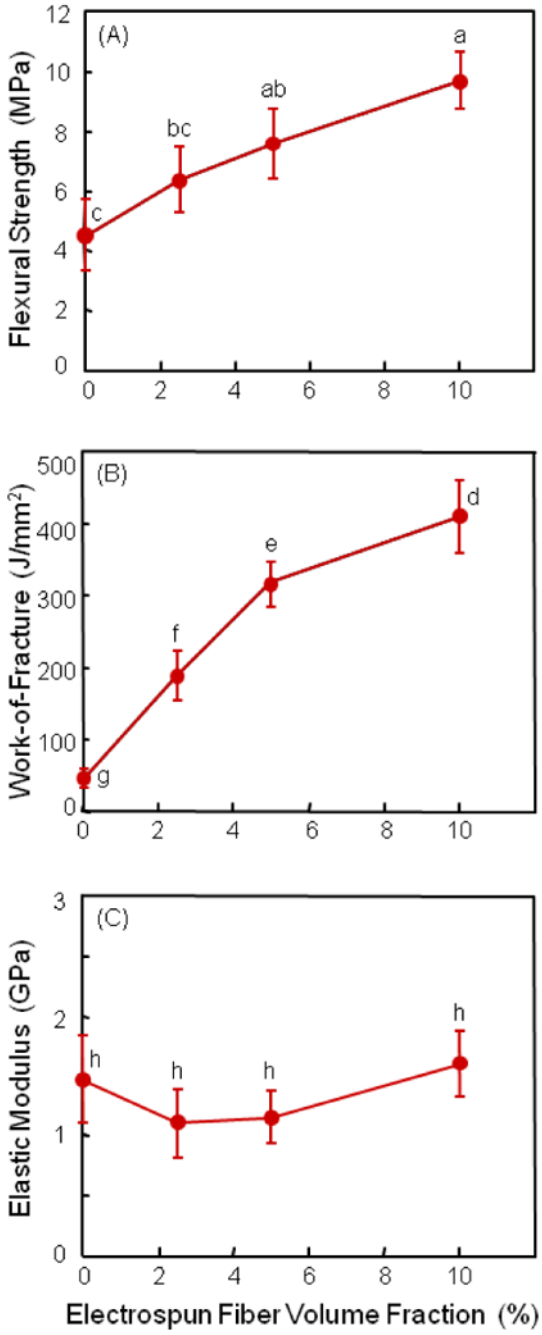

[2].
Mechanical properties vs. electrospun fiber volume fraction in CPC. (A) Flexural strength, (B) work-of-fraction (toughness), and (C) elastic modulus. Each value is the mean of six measurements with the error bar showing one standard deviation (mean ± sd; n = 6). In each plot, values indicated with dissimilar letters are significantly different from each other ($p < 0.05$). For example, “a” is not significantly different from “ab” ($p > 0.1$); however, “a” is significantly different from “bc” and “c” ($p < 0.05$).

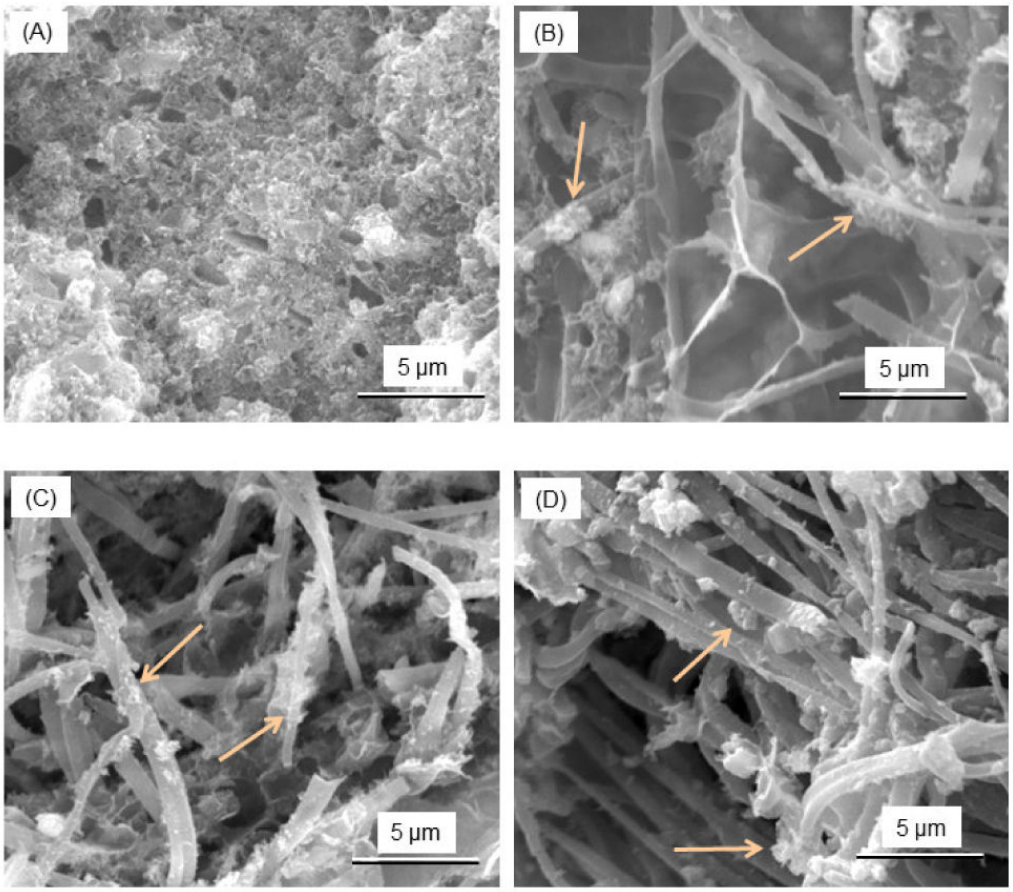

[3].
SEM of electrospun fiber-CPC specimen surfaces with fiber volume fractions of (A) 0%, (B) 2.5%, (C) 5%, and (D) 10%. The electrospun PLGA fibers were mixed well with the CPC paste. CPC appeared to be bonded onto the fiber surfaces. Arrows indicate the CPC materials that were adherent on the fiber surfaces.

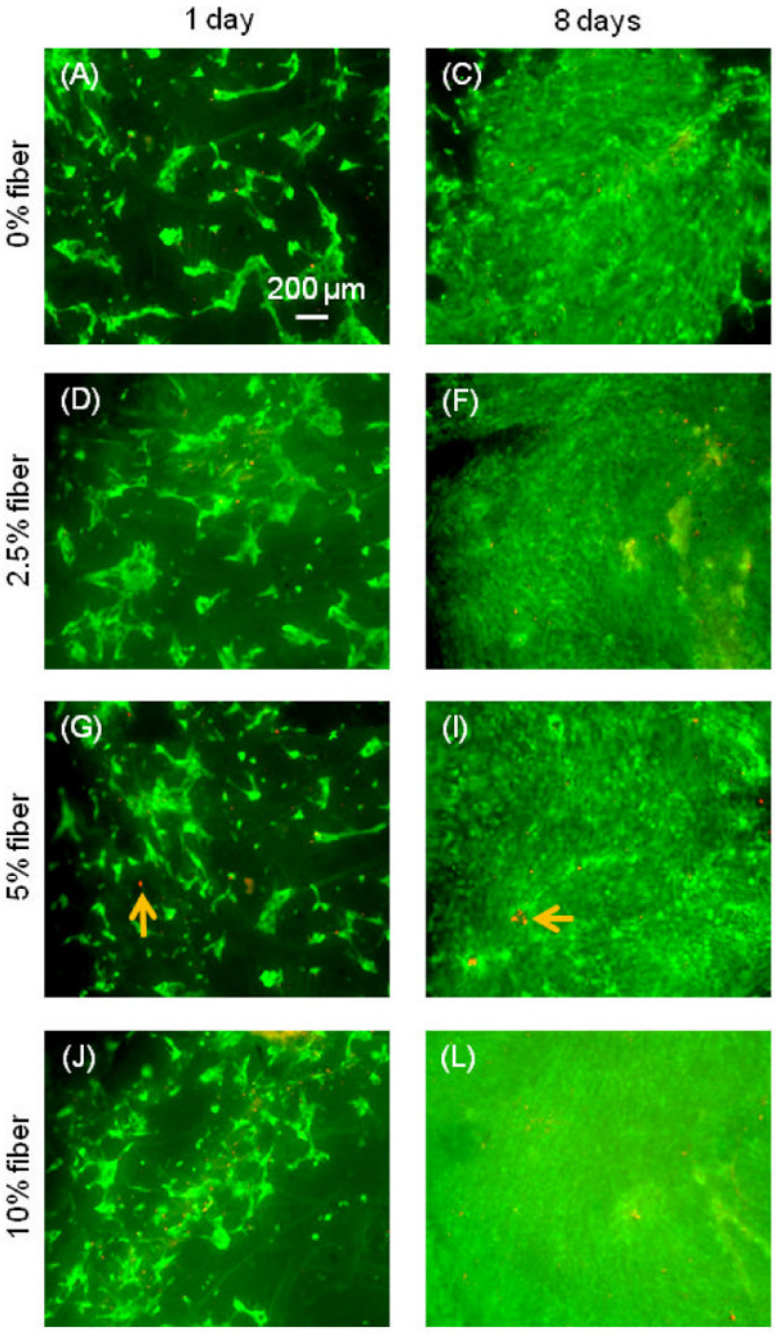

[4].
Live/dead assay photos of hUCMSCs on electrospun fiber-CPC scaffolds. The time periods are listed on the top of the figure. The PLGA fiber volume fractions in CPC are listed on the left side. Live cells were stained green and were numerous. Dead cells were stained a red/orange color and were few (arrows indicate examples).

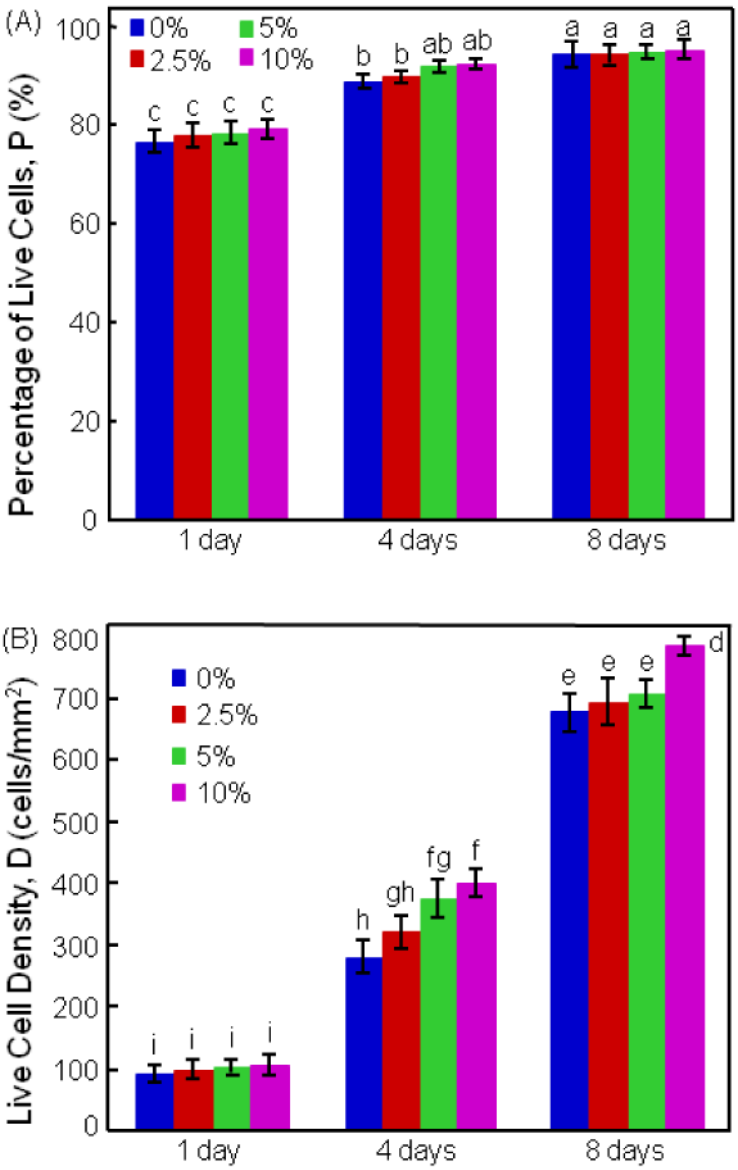

[5].
hUCMSC viability on electrospun fiber-CPC scaffolds. (A) Percentage of live cells, P. (B) Live cell density, D. Each value is mean ± sd; n = 5. In each plot, values indicated with dissimilar letters are significantly different from each other ($p < 0.05$). The legend in the plot indicates the PLGA fiber volume fraction in CPC.

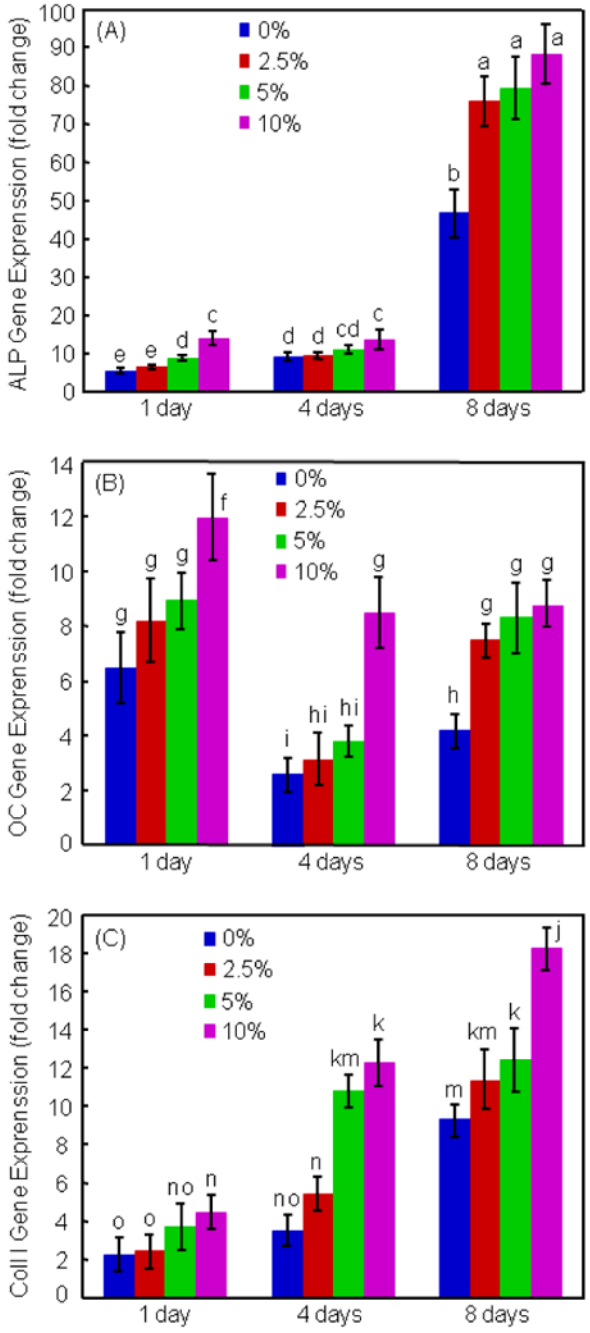

[6].

Osteogenic differentiation of hUCMSCs on electrospun fiber-CPC: (A) ALP, (B) OC, and (C) collagen I gene expressions, measured by the RT-PCR method. Each value is mean ± sd; n = 5. In each plot, values indicated with dissimilar letters are significantly different from each other ($p < 0.05$). The legend in the plot indicates the PLGA fiber volume fraction in CPC. Adding submicron PLGA fibers to CPC significantly increased the osteogenic gene expressions of the hUCMSCs.

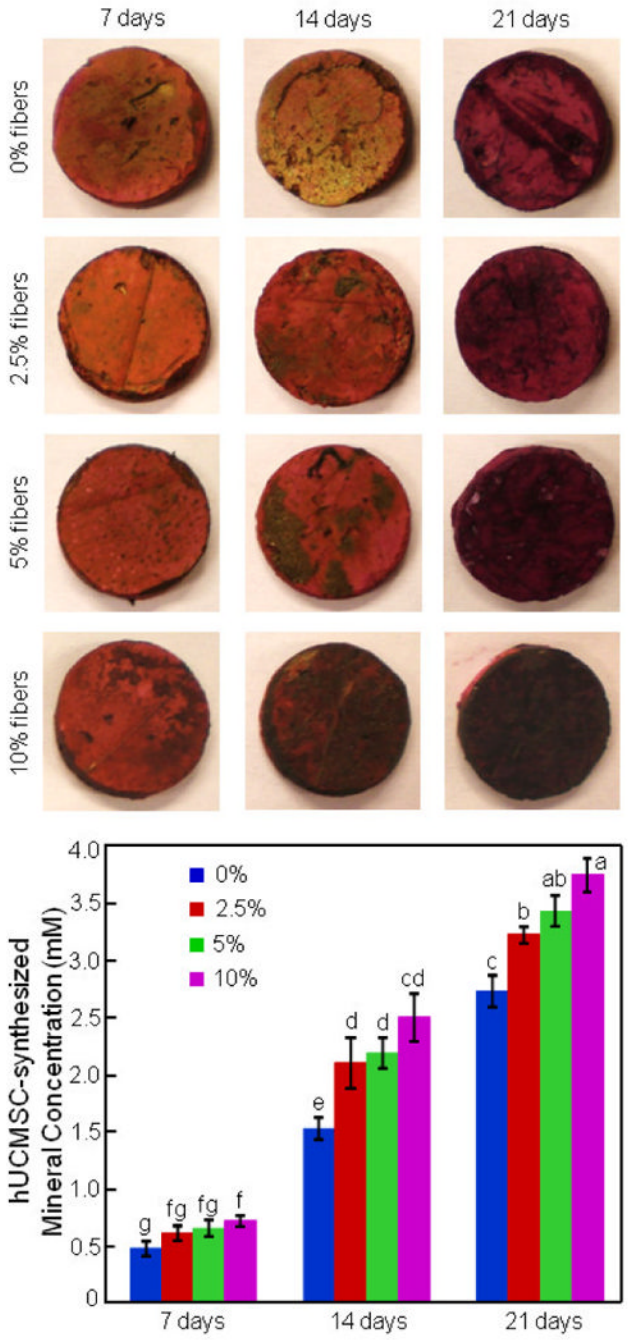

[7].
hUCMSC mineralization while attaching on the electrospun fiber-CPC scaffolds. The photos are for hUCMSC seeding on the fiber-CPC, with fiber volume fractions listed at the left side, and culture time listed on the top. The data from the osteogenesis assay are shown in the plot (mean ± sd; n = 5). In each plot, values indicated with dissimilar letters are significantly different from each other ($p < 0.05$). The mineral amount increased with culture time, as well as with the fiber volume fraction in CPC.